Extended Abstracts of the 2015 International Conference on Solid State Devices and Materials, Sapporo, 2015, pp482-483

Axial Strain Effects on Phonon Thermal Transport in Silicon Nanowires

Junichi Hattori, Vladimir Poborchii, and Tetsuya Tada

Nanoelectronics Research Institute, National Institute of Advanced Industrial Science and Technology
1-1-1 Umezono, Tsukuba, Ibaraki 305-8568, Japan
Phone: +81-29-861-3121, E-mail: j.hattori@aist.go.jp

We study the phonon thermal transport in axially strained silicon nanowires (Si NWs) using an atomistic approach. In the ballistic limit, the compressive (tensile) axial strain improves (reduces) thermal transport properties in [001]-oriented Si NWs, while in the diffusive limit, it reduces (improves) the properties. The relation between these strain effects and the wire size or orientation is also investigated.

1. Introduction

Silicon Nanowires (Si NWs) have been attracting widespread attention as a promising material for a variety of applications such as ultra-scaled transistors [1] and thermoelectric (TE) devices [2]. The two devices require contrasting thermal transport properties of the channel material. For semiconductor transistors the properties should be high to suppress the self-heating effects [3], while for TE devices they should be low to effectively convert between thermal gradients and electric fields. Thus, a method to control the properties will be highly beneficial. As for carrier transport properties, strains are commonly used to improve them of Si channels in transistors [4]. The strain effects on thermal transport properties in Si NWs, however, have not yet been well understood and it might be even difficult to assess the possibility of strain control of the properties. In this work, we study theoretically the phonon contribution to thermal transport in Si NWs under strains along the wire axis. The phonon thermal transport in such axially strained Si NWs has recently been investigated using molecular dynamics simulation [5] and using a lattice dynamics approach [6]. In the lattice dynamics approach, the strain effects on phonon thermal transport appear only through phonon dispersion relations, which is helpful for us to analyze and understand the strain effects. Thus, we also adopt a similar approach. Although, in the previous work [6], the strain-induced deformation of Si NWs was assumed to be the same as that of bulk Si, they both must be different from each other because the NWs have interfaces. To clarify the whole picture of the strain effects, we estimate the actual deformation of the axially strained Si NWs by performing structural relaxations.

2. Phonon Dispersion Relation

We first considered a [100]-oriented Si NW having a square cross section with a side length of 3 nm [Fig. 1(a)]. The potential energy of the NW, U, was approximated as the sum of the potential energies due to interactions between the constituent atoms, and the interaction potential energies were evaluated with the Stillinger–Weber model [7]. The atomistic structure of the NW under a given axial strain, ϵ_{zz}, can be determined by moving the atoms in the unit cell of the NW to the positions where U takes a local minimum, after enlarging the unit cell along the wire axis by a factor of $(1 + \epsilon_{zz})$. To find the atomic positions, we used the numerical optimization technique, the limited-memory BFGS method with an Armijo rule [8]. Conducting the lattice dynamics calculation [9] with the resulting atomistic structure, we can obtain the phonon dispersion relation in the NW. Figure 2 shows the dispersion relations in the [100]-oriented Si NWs with different ϵ_{zz}'s. For the compressive (tensile) strain, the dispersion relation is scaled up (down) in terms of the phonon frequency, ω. This is mainly because the atomic bonds in the NW become short (long) and accordingly the force constants for bond stretching increase (decrease), as shown in Fig. 3. As to bond angles, since some are bent and the others unbent, the average angle changes very little, as shown in Fig. 4(a). Nevertheless, the force constants for bond angle bending show the same strain dependence as the bond stretching ones, on average, which is shown in Fig. 4(b).

3. Phonon Thermal Transport

We calculated the thermal conductance in the ballistic limit [10], K_{bal}, in the [100]-oriented Si NWs with the previously obtained phonon dispersion relations. The resulting K_{bal} is shown in Fig. 5 as a function of the axial strain ϵ_{zz}, from which it can be seen that the compressive (tensile) strain increases (decreases) K_{bal}. This increase (decrease) in K_{bal} stems from that in the phonon group velocity, v, due to the scale up (down) of the dispersion relation in terms of ω. We also examined the thermal transport in the diffusive limit with respect to thermal conductivity. Figure 7 shows the diffusive thermal conductivity [10], κ_{dif}, in the [100]-oriented Si NWs. Here, the three phonon scattering mechanisms, Umklapp, second order three-phonon, and boundary scattering [11] were taken into account. As can be seen from the Figs. 5 and 7, the ϵ_{zz}-dependence of κ_{dif} is opposite to that of K_{bal}. The increases in ω and v lead to those in the Umklapp and boundary scattering rates, respectively. For this reason, if $\epsilon_{zz} < 0$, κ_{dif} reduces, and vice versa.

4. Influence of Wire Size/Orientation on the Strain Effects

Figures 6(a) and 8(a) show K_{bal} and κ_{dif} in [100]-oriented square Si NWs with different side lengths. Except for the case of the finest NW, the figures indicate that the strain effects on K_{bal} and κ_{dif} are almost independent of the wire size. Also, Figs. 6(b) and 8(b) show K_{bal} and κ_{dif} in the [110]- and [111]-oriented NWs [Figs. 1(b) and 1(c)]. The ϵ_{zz}-dependence of K_{bal} and κ_{dif} in the two NWs differs obviously from that in the [100]-oriented NW. The root cause is the disorder in bond stretching force constants, which stems from the simultaneous presence of bonds stretched and contracted by the strain.

5. Conclusions

We have studied theoretically the phonon thermal transport in axially strained Si NWs using a lattice dynamics approach. In the [100]-oriented NWs, the compressive (tensile) strains improve (reduce) the ballistic thermal conductance, while reduce (improve) the diffusive thermal conductivity. It was also found that although the strain effects only slightly depend on the wire size, they change fundamentally with the wire orientation.

References

[1] N. Singh *et al.*, IEEE Electron Device Lett. **27**, 383 (2006).
[2] A. I. Boukai *et al.*, Nature **451**, 168 (2008).
[3] R. Wang *et al.*, IEEE Electron Device Lett. **30**, 559 (2009).
[4] N. Mohta and S. E. Thompson, IEEE Circuits & Devices Mag. **21** [5], 18 (2005).
[5] X. Li *et al.*, Phys. Rev. B, **81**, 245318 (2010).
[6] A. Paul and G. Klimeck, Appl. Phys. Lett. **99**, 083115 (2011).
[7] F. H. Stillinger and T. A. Weber, Phys. Rev. B **31**, 5262 (1985).
[8] J. Nocedal and S. J. Wright, *Numerical Optimization* (Springer, New York, 1999) p. 224.
[9] A. Paul *et al.*, J. Comput. Electron. **9**, 160 (2010).
[10] J. Hattori and S. Uno, Jpn. J. Appl. Phys. **52**, 04CN04 (2013).
[11] H. Karamitaheri *et al.*, J. Electron. Matter. **43**, 1829 (2013).

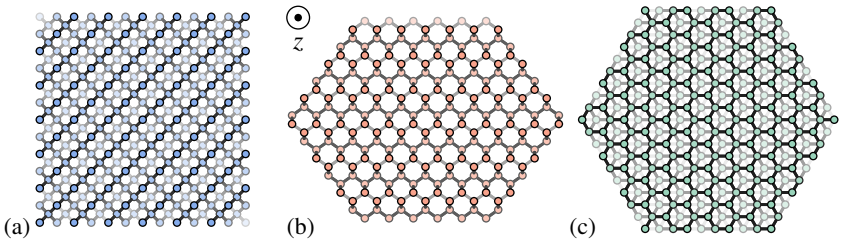

Fig. 1. Schematic top views of cross sections of (a) the [100]-, (b) [110]-, and (c) [111]-oriented Si NWs considered in this study. The areas of the three cross sections without any strain, A_0's, are about 3.274×3.274 (≈ 10.72), 10.11, and 10.45 nm^2. Also, an axis of a Cartesian coordinate system was placed along the NW axis and is referred to as z-axis.

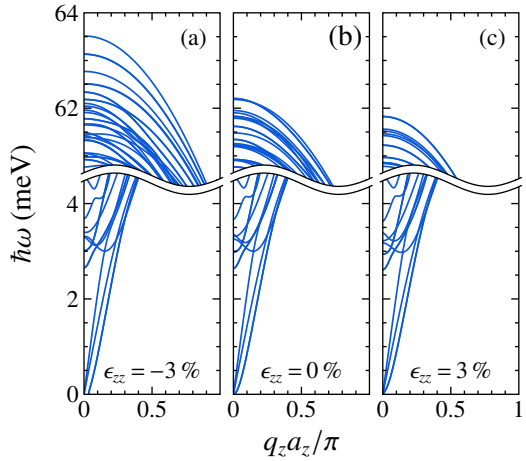

Fig. 2. Phonon dispersion relations in [001]-oriented Si NWs under an axial strain ϵ_{zz} of (a) −0.03, (b) 0, and (c) 0.03. The horizontal axes represent the phonon wavevector along the z-axis, q_z, and the vertical axes the phonon energy, $\hbar\omega$.

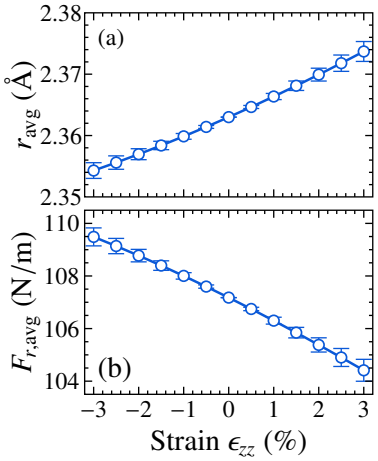

Fig. 3. (a) Average bond length in a [001]-oriented Si NW, plotted as a function of the strain. (b) Same as in (a) but for the average force constant for bond stretching.

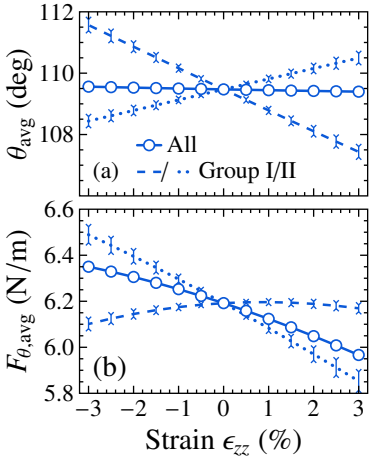

Fig. 4. Same as in Fig. 3 but for (a) the average bond angle and (b) average force constant for bond angle bending. In [001]-oriented Si NWs, bond angles can be divided into two groups based on relative positions of their constituent atoms along the z-axis.

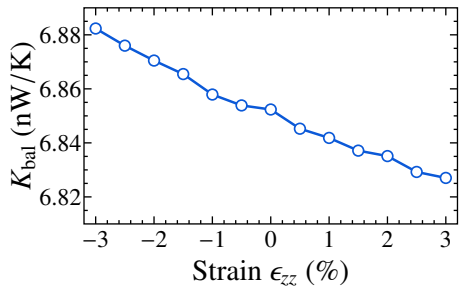

Fig. 5. Ballistic thermal conductance K_{bal} in [001]-oriented Si NWs under different strains at a temperature of 300 K.

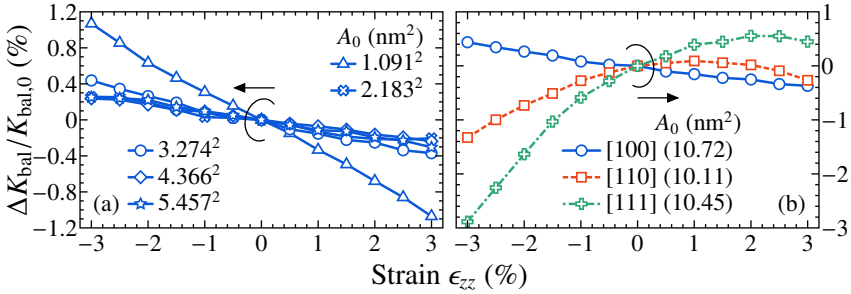

Fig. 6. Variation in K_{bal} with the strain, calculated for (a) [001]-oriented square Si NWs with different A_0's and (b) Si NWs with different wire orientations. The vertical axes are normalized by K_{bal} in the corresponding unstrained Si NW.

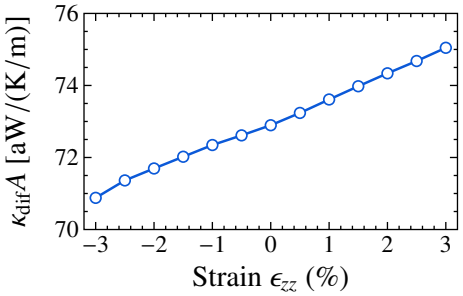

Fig. 7. Diffusive thermal conductivity κ_{dif} multiplied by the cross-sectional area A in [001]-oriented Si NWs under different strains at 300 K.

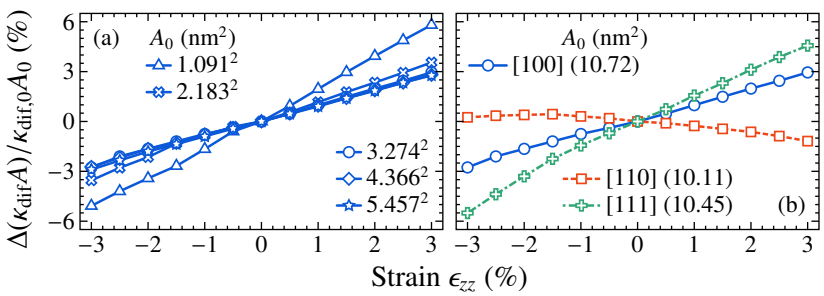

Fig. 8. Variation in $\kappa_{dif}A$ with the strain, calculated for (a) [001]-oriented square Si NWs with different A_0's and (b) Si NWs with different wire orientations. The vertical axes are normalized by the value of $\kappa_{dif}A$ in the corresponding unstrained Si NW.